B.I. Kuznetsov, T.B. Nikitina, I.V. Bovdui, K.V. Chunikhin, V.V. Kolomiets, B.B. Kobylianskyi

Optimization of combined active-passive electromagnetic shielding system for overhead power lines magnetic field normalization in residential building space

Problem. *Normalization of overhead power lines magnetic field level in residential building.* ***Goal.*** *Normalization of overhead power line magnetic field by optimization of combined electromagnetic shielding system, consisting of active and passive parts, in residential building space based on magnetic field three-dimensional model.* ***Methodology.*** *Optimization of combined electromagnetic shielding system for initial magnetic field three-dimensional model solved based on multi-criteria two-player antagonistic game solution. Game payoff vector calculated based on finite element calculations system COMSOL Multiphysics package. Game solution calculated based on particles multiswarm optimization algorithms.* ***Results.*** *The results of theoretical and experimental studies of combined electromagnetic passive and active shielding system for magnetic field three-dimensional model in residential building from two-circuit overhead power transmission line with wires «Barrel» type arrangement presented.* ***Scientific novelty.*** *For the first time the method for normalization of overhead power lines magnetic field in residential building space based on optimization of combined active-passive electromagnetic shielding system for magnetic field three-dimensional model developed.* ***Practical value.*** *Spatial location coordinates of shielding winding, currents and phases in shielding winding of robust active shielding system, geometric dimensions and thickness of electromagnetic passive shield calculated during optimization of combined electromagnetic shielding system for magnetic field three-dimensional model. References 49, figures 13.*
Key words: **overhead power line, magnetic field, combined electromagnetic active and passive shielding system, computer simulation, experimental research.**

Проблема. Нормалізація рівня магнітного поля повітряних ліній електропередачі в житлових будинках. Мета. Нормалізація рівня магнітного поля повітряних ліній електропередачі шляхом оптимізації комбінованої електромагнітної екрануючої системи, що складається з активної та пасивної частин, у просторі житлових приміщень на основі тривимірної моделі магнітного поля. Методологія. Оптимізація комбінованої електромагнітної екрануючої системи тривимірної моделі вихідного магнітного поля розраховується на основі рішення багатокритеріальної антагоністичної гри двох гравців. Вектор виграшів гри розраховується на основі кінцево-елементної системи обчислень COMSOL Multiphysics. Рішення гри розраховується на основі алгоритмів оптимізації мультироїв частинок. Результати. Наведено результати теоретичних та експериментальних досліджень комбінованої електромагнітної системи пасивного та активного екранування тривимірної моделі магнітного поля в житловому будинку від дволанцюгової повітряної лінії електропередач із розташуванням проводів типу «бочка». Наукова новизна. Вперше розроблено метод нормалізації магнітного поля повітряних ліній електропередачі в житловому приміщенні на основі оптимізації комбінованої активно-пасивної системи електромагнітного екранування тривимірної моделі магнітного поля. Практична значимість. Координати розташування екрануючих обмоток, струм і фаза в екрануючих обмотках робастної системи активного екранування, та геометричні розміри і товщина електромагнітного пасивного екрану розраховуються при оптимізації комбінованих електромагнітних екрануючих систем тривимірної моделі магнітного поля. Бібл. 49, рис. 13.
Ключові слова: **повітряна лінія електропередачі, магнітне поле, комбінована електромагнітна активна та пасивна система екранування, комп'ютерне моделювання, експериментальні дослідження.**

Introduction. Many residential buildings in Ukraine are located in close proximity to overhead power lines. Induction level in such houses is many times higher than modern standards for industrial frequency magnetic induction level for safe living [1–3].

Most often, single-circuit power lines with a triangular arrangement of wires located near single-story old buildings. Double-circuit power lines with a «Barrel» type of wire arrangement also often located near single-story and multi-story residential buildings of old construction, as shown in Fig. 1.

Fig. 1. A multi-storeys residential building located near a double-circuit power line

One of most economically justified approaches to further operation of high-grade residential buildings without eviction of population or replacement of existing overhead power lines with underground cable power lines used of original magnetic field modeling and shielding to safe level for habitation [4–7].

To implement necessary shielding factor of initial magnetic field, it is necessary to use active shielding [8–18]. To increase the effectiveness of shielding, especially in long-distance residential buildings, it is advisable to use combined shielding of the initial magnetic field, including active and passive shielding [19].

The diagram of such combined electromagnetic active-passive shielding system shown in Fig. 2.

The active shielding system contains shielding windings, amplifier, control system and a magnetic field sensor installed inside the shielding space. An external power source used to power the active shielding system.

This magnetic field sensor, which installed inside the shielding space, measured resulting magnetic field generated by power line and combined electromagnetic active-passive shielding system inside shielding space.

The source of energy for passive shielding system is the external electromagnetic field acting on the passive electromagnetic shield. This external magnetic field for

the passive shield generated by power transmission line wires and compensation windings of electromagnetic active shielding system. Under the influence of this primary magnetic field, currents induced in the passive electromagnetic shield, which create a secondary magnetic field. This secondary magnetic field directed opposite to the original primary field.
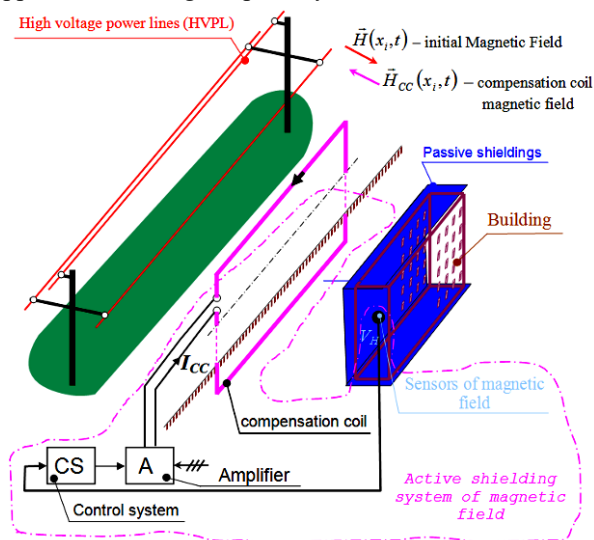

Fig. 2. Combined electromagnetic active-passive shielding system diagram

The resulting magnetic field, which is equal to the sum of the primary magnetic field generated by power transmission line wires and compensation windings, and the secondary magnetic field generated by the passive screen, will be less than the initial magnetic field. Due to this reduction in the resulting magnetic field, the shielding effect of the combined active-passive electromagnetic shielding system achieved.

Note that since the active and passive shielding systems influence each other, when optimizing the combined active-passive electromagnetic shielding system, it is necessary simultaneously optimize both the parameters of the active and the parameters of the passive electromagnetic system to achieve the minimum resulting magnetic field in the shielding space.

Often, to increase the efficiency of shielding the original magnetic field using such hybrid electromagnetic active-passive shielding system, the active shielding system designed as a system with two degrees of freedom. In this case, two closed and open control loops used simultaneously. To implement open-loop control, another magnetic field sensor used to measure the initial magnetic field, which installed outside the shielding space. This magnetic field sensor usually installed away from the shielding space but close to power transmission line wires in order to reduce the influence of compensation winding currents of active shielding system.

When designing electromagnetic shielding systems, two geometric problems of magnetostatic's solved [12, 13]. First, a geometric forward problem of magnetostatics solved when, for given values and geometric arrangement of sources of industrial frequency magnetic field, the magnetic field induction calculated at given points of the shielding space. This geometric forward problem calculated effect from magnetic field source of a given power and located in a given «geometric» position at points in the shielding space.

The geometric inverse problem of magnetostatics calculate the power and «geometric» position of industrial frequency magnetic field sources that generate a given magnetic field at given points in the shielding space. Thus, in the course of solving a geometric inverse problem, it is necessary to calculate not the result, but the cause that leads to a given result. Naturally, a geometric inverse problem is an uncorrected problem and can have many solutions. As a rule, solving a geometric inverse problem reduced to solving an optimization problem [20–23].

The work [19] considered issues of synthesis of systems for combined magnetic field shielding in a two-dimensional formulation. In this case, shielding is assumed in the central section of residential buildings.

However, when magnetic field shielding in residential buildings, it is necessary to reduce magnetic field induction level to a safe level in apartments located at edges of house.

Most studies carried out based on two-dimensional magnetic field model, which does not allow studying effectiveness decrease of original field shielding in residential building edges [8–18]. This determines the formulation and solution of problem of design of combined electromagnetic active-passive shielding system in three-dimensional formulation.

The **goal** of the work is normalization of overhead power line magnetic field by optimization of combined electromagnetic shielding system, consisting of active and passive parts, in residential building space based on magnetic field three-dimensional model.

Definition of geometric forward magnetostatic problem for overhead power lines and compensating winding magnetic field. Geometric forward magnetostatic problem calculates the consequence – the magnetic field at a given point in space, generated by a given source of magnetic field located at a given «geometric» point in space. This problem is solved on basis of Maxwell's law is a mathematically correct problem and calculated exactly.

Geometric forward magnetostatic problem for overhead power lines and compensating winding magnetic field is to calculate magnetic field at any point in space for given magnetic field sources. Mathematical modeling of magnetic field reduced to boundary value problem solution for electromagnetic field with a known distribution of its sources in the volume or on the surface of the given area [4–6]. To correctly solve this problem, it is necessary, first of all, to choose a physical model of this process, which covers its main aspects. Physical model should be one of Maxwell equations full system simplifications. Maxwell equations describing electromagnetic fields in media with continuous or piecewise-continuously changing properties are the basis for analytical and numerical modeling of any electromagnetic processes, both in vacuum and in material media [7].

To simplify high-voltage power transmission lines magnetic field mathematical mode, the phase's wires taken in infinite long form and thin straight conductors, which allows two-dimensional magnetic field model used which contains two spatial components along axes and does not depend on coordinate along which power line wires conductors located. However, in this task, controlled windings vertical sections of active shielding system create significant projections of magnetic field intensity vector, which constitute, along coordinate , which determines

three-dimensional magnetic field model used. Such model, in addition, also allows take into account magnetic field intensity vector component along coordinate, created by power lines due to their sagging between supports.

When calculating current magnetic field quasi-static approximation of Maxwell equations system [4–7] is equivalent to Biot-Savart's law, which can written in form [4]:

$$\boldsymbol{B}(P) = \frac{\mu_0 I_m}{4\pi} \int\limits_L \frac{[\mathrm{d}\boldsymbol{l} \times \boldsymbol{R}]}{R^3}, \qquad (1)$$

where $\boldsymbol{B}(P)$ – magnetic field induction at observation point P; $\mathrm{d}l$ – circuit element with current I_m; $\boldsymbol{R}$ – vector directed from contour element $\mathrm{d}l$ to observation point P.

Definition of forward quasi-static magnetic field active shielding system design problem. Let us consider definition of forward quasi-static magnetic field active shielding system design problem. Forward magnetic field active shielding system design problem calculated magnetic field induction generated by the compensation windings in shielding space given point for given compensation windings spatial location coordinates of active shielding system.

First, consider geometric direct problem solution for power lines – mathematical model design of initial magnetic field generated by power transmission line. Power lines wires position initially known. Power lines wires instantaneous values currents set in dependences sinusoidal form. We set amplitudes A_i and phases φ_l of industrial frequency currents of power line wires. Let's set power transmission lines wire currents in complex form

$$I_i(t) = A_i \exp j(\omega t + \varphi_i). \qquad (2)$$

Then, based on relation (1), initial magnetic field induction $\boldsymbol{B}_0(P_i,\boldsymbol{I}_0(t),t)$ at point P created by power transmission lines currents calculated in following form

$$\boldsymbol{B}_0(P_i,\boldsymbol{I}_0(t),t) = \sum\limits_{l=1}^{L} \boldsymbol{B}_{0l}(P_i,I_l(t)). \qquad (3)$$

Power line currents vector $\boldsymbol{I}_0(t)$ introduced components of which are power line wires currents

$$\boldsymbol{I}_0(t) = \{I_l(t)\}.$$

Note that when transmission line resulting magnetic field calculating according to (1) for 3D modeling, it is necessary to take into account the real sagging of transmission line wires, and elementary sections number of transmission line conductors at ends of considered sections of transmission lines must be determined from required accuracy of resulting magnetic field induction calculation, which generated by all power lines at given point in shielding space.

Let us now consider forward problem solution for calculating magnetic field generated by compensation windings at shielding space points. Let us set compensating windings location coordinates of active shielding system in form of initial geometric values vector of compensating windings dimensions of active protection, as well as amplitude A_i and phase φ_l of compensating windings currents [12–14]. Let's set compensating windings currents in complex form

$$I_{ai}(t) = A_{ai} \exp j(\omega t + \varphi_{wi}). \qquad (4)$$

Then, based on (1) similar to (3) magnetic field induction at point P_i created by windings currents at time moment t calculated in the following form

$$\boldsymbol{B}_y(P_i,\boldsymbol{I}_y(t),t) = \sum\limits_{m=1}^{M} \boldsymbol{B}_{ym}(P_i,I_{ym}(t),t), \qquad (5)$$

here currents vector $\boldsymbol{I}_y(t)$ in compensating windings introduced with windings currents components

$$\boldsymbol{I}_y(t) = \{I_{ym}(t)\}.$$

Note that when calculating resulting magnetic field generated by all compensating windings wires, according to formula (5), for 3D modeling, it is necessary to take into account not only real dimensions of horizontal parts of compensating windings, but also real length of compensating windings, since it is near ends of horizontal sections of compensating windings that greatest change in magnetic field induction level generated by compensating windings is observed.

Naturally, that in 3D modeling in (5) it is necessary to take into account vertical parts of compensating windings, since it is these vertical parts that generate main part of the of the magnetic field induction level.

Then, based on superposition principle, the resulting magnetic field induction vector $\boldsymbol{B}(P_i,\boldsymbol{I}_0(t),\boldsymbol{I}_y(t),t)$ at the point P_i, created by power line wires currents (1) and controlling windings currents (5), is equal to vectors sum [4]

$$\boldsymbol{B}(P_i,\boldsymbol{I}_0(t),\boldsymbol{I}_y(t),t) = \boldsymbol{B}_0(P_i,\boldsymbol{I}_0(t),t) + \ldots + \boldsymbol{B}_y(P_i,\boldsymbol{I}_y(t),t). \ (6)$$

Definition of forward dynamic problem of magnetic field active shielding system design. The calculation of the magnetic field generated by the transmission line wires and compensation windings calculated based on the Biot-Savart's law [4–7]. In this case, the magnetic field induction is a static dependence (1) on the current of the transmission line wires or compensation windings. Thus, the magnetic field is practically «instantaneously» generated by currents and the speed of propagation of the electromagnetic field of industrial frequency is neglected.

However, the active shielding system is a dynamic system, the processes in which are commensurate with the industrial frequency. Moreover, the design of the active shielding system performed taking into account the dynamic characteristics of its elements - the presence of inductances of compensating windings, the presence of time delay of magnetic field sensors and other. In the active shielding system with two degrees of freedom, open-loop control by disturbance and closed-loop control by deviation with the help of feedback used simultaneously.

The forward problem of dynamic magnetic field active shielding system is the calculation of the dynamic characteristics of the active shielding system with two degrees of freedom for the given values of the parameters of the open-loop and closed-loop control regulators and for the given values of the parameters of the disturbing effects and interference measurements of the sensors of the initial and resulting magnetic field, with the help of which the open-loop and closed-loop control is implemented. This forward dynamics problem of an active shielding system is a correct mathematical problem and solved «exactly», for example, by direct modeling of processes in such a dynamic system with two degrees of freedom.

The inverse dynamics problem of an active shielding system consists in calculating the values of the parameters of the open-loop and closed-loop control regulators for the given values of the parameters of the disturbing effects and the interference of the measurements of

magnetic field sensors of initial and resulting magnetic field for implementation of specified dynamic characteristics in designed system. The solution of the inverse problem of the dynamics of an active shielding system reduced to an optimization problem.

In this case, the open and closed control channel regulators synthesized from the condition of minimizing the error of compensation of the initial magnetic field, caused by the disturbing effect in the form of induction of the initial magnetic field. In this case, with the help of these same open and closed control regulators, the noise of the magnetic field sensors measuring the initial magnetic field and the resulting magnetic field in the shielding space filtered.

The inverse dynamics problem of active shielding system is an uncorrected mathematical problem, and its solution is also found approximately by numerical methods. One of the possible approaches to solving the inverse problem of dynamics for active shielding system with two degrees of freedom control used of robust optimal control based on four Riccati equations solutions [24–26]. To implement such robust optimal control, robust optimal Kalman's filters used, which also synthesized based on four Riccati equations solutions [26–28].

Such a robust optimal solution to the inverse dynamics problem for active shielding system with two degrees of freedom control allows obtained the highest accuracy of the active shielding system; however, the implementation of such a system presents certain difficulties. Therefore, the overwhelming majority of industrial control systems built on the principle of subordinate regulation and implemented using standard PID controllers.

Let us accept the structure of the active shielding system as two-loop subordinate control system. The internal loop of such a system is the current control loop of the compensation winding. With the help of the PI controller of the current loop, the «large» time constant of the current loop, caused by the inductance of the compensation winding, compensated. The external loop of this two-loop subordinate control system is the loop for regulating the induction of the resulting magnetic field.

A delay link used to form open-loop control for active shielding system with two degrees of freedom control over the initial magnetic field. The magnitude of the gain and delay coefficients experimentally adjusted during the system setup from the condition of minimizing the space-time characteristic of the resulting magnetic field in the shielding space.

Let us consider definition of forward magnetic field active shielding dynamic system design problem. Forward dynamic magnetic field active shielding system design problem calculated magnetic field induction generated by the compensation windings in shielding space given point not for given compensation windings spatial location coordinates but and for given structure and parameters of active shielding system regulators as closed loop and open loop dynamic system [20–23]. This dynamic active shielding system is two degrees of freedom dynamic system. This dynamic system combines both open loop and closed-loop control. However, in contrast to classical synthesis of robust control system with two degrees of freedom, in the developed method, the synthesis of open-loop coarse control performed based on quasi-static model of magnetic field. Synthesis of closed-loop refinement control carried out based on closed system dynamics

equations, taking into account plant models and measuring equations devices, disturbances and measurement noise.

First, consider the possible structures of dynamic magnetic field active shielding system design problem. If it is possible to measure the of the power line wires current of three-phase power lines or directly measure magnetic field induction near power line wires , then can design open loop system of dynamic magnetic field active shielding system as follows.

Initial magnetic field model in considered space can be taken in form of magnetic field generated by three, six, and etc. conductors of three-phase current of industrial frequency, located in known position relative to considered space, in which it is necessary shielded magnetic field.

To design open loop control circuit of magnetic field active shielding system sufficient measured current wires current line one phase and used some reference voltage

$$u_u(t) = A_u \sin(\omega t + \varphi_u). \qquad (7)$$

Based on measured wires current line as reference voltage, we will form open loop control by compensation windings current at following form

$$u_i(t) = A_i \sin(\omega t + \varphi_i) + f_{uI}, \qquad (8)$$

where A_i – the sought amplitudes and φ_i – control phases in the i-th compensation windings current with respect to the measured current in the phase of the current line or reference voltage; f_{ui} – equivalent noise of current or reference voltage measurement.

It is advisable to supplement such open loop control circuit with feedback control circuit, so that the active shielding system becomes two degrees of freedom dynamic system one based on control principle.

To design closed loop control by active shielding system, it is necessary to have magnetic field induction measuring devices – magnetometers installed at certain points in space to measure resulting magnetic field induction created by both power line wires current and compensation windings current of active shielding system. Let's form a vector $\mathbf{y}(t)$ of measured components of resulting magnetic field induction vector at some points P_j

$$\mathbf{v}(t) = \left\{ \mathbf{B}_0\left(P_j, \mathbf{I}_0(t), t\right) + \mathbf{B}_y\left(P_j, \mathbf{I}_y(t), t\right) \right\} \qquad (9)$$

at time moment t at magnetometers installation points P_j in following form

$$\mathbf{y}(t) = \mathbf{v}(t) + \mathbf{w}(t), \qquad (10)$$

where $\mathbf{w}(t)$ – magnetometer noise vector.

Note that when using combined shielding resulting magnetic field, simultaneously generated by power line wires, compensation windings wires of active shielding system and passive shield, measured by magnetometer installed in shielding space point [19].

Let's take structure of closed loop control by active shielding system of magnetic field in following form: we will apply corresponding magnetometer output voltage to each channel PID controller input.

Let's write down state differential equation of discrete PID regulators, the input of which is vector $\mathbf{y}(t)$ of measured magnetic field induction components, and output is closed-loop control vector $\mathbf{u}_3(t)$ of compensation windings wires in the following form

$$\mathbf{x}_p(t+1) = A_p \mathbf{x}_p(t) + B_p \mathbf{y}(t); \qquad (11)$$

$$\mathbf{u}_3(t) = C_p \mathbf{x}_p(t) + D_p \mathbf{y}(t), \qquad (12)$$

in which elements of matrices A_p, B_p, C_p, D_p calculated by PID regulators parameters.

Then design of two degrees of freedom dynamic system of active shielding of magnetic field, which includes open and closed control loops reduced to calculated regulators parameters vector, components of which are sought elements of matrices A_p, B_p, C_p, D_p, determined by closed control channels PID regulators gain coefficients, as well as vector of sought amplitudes $A = \{A_i\}$ and phases $\boldsymbol{\varphi} = \{\varphi_i\}$ of compensation windings wires currents, components of which are amplitudes A_i and currents φ_i of components of compensation windings wires currents open loop control regulators [24–26].

Definition of geometric forward magnetostatic problem for passive electromagnetic shielding magnetic field. Let us now consider geometric forward problem of magnetostatics for a continuous electromagnetic passive shield. The geometric forward problem for a passive electromagnetic shield also calculates the consequence – the magnetic field at a given point in space, generated by a given source of magnetic field in form of passive shield, located at a given «geometric» point in space. This problem is also solved on basis of Maxwell's law and is mathematically correct problem and calculated exactly [4–7].

The principle of operation of a passive electromagnetic shield based on action of the initial primary magnetic field, as a result of which conduction currents induced in the passive screen. These currents create a secondary magnetic field, which, according to Faraday's law, directed opposite to the initial magnetic field. The resulting magnetic field, equal to the sum of the primary and secondary fields, is weaker than the primary field in the protected area, due to which the initial magnetic field shielded.

The general approach to solving magnetic field shielding problems using a passive electromagnetic shield also comes down to integrating Maxwell's equations in all areas: both inside the shield volume and in the external environment. When considering the problems of shielding industrial frequency magnetic field, Maxwell's equations solved in a quasi-stationary approximation. In the numerical solution, the space divided into simply connected dielectric regions, the boundaries of which are conducting shells. The finite element method has received the greatest distribution for numerical study of electromagnetic field.

The numerical procedure reduced to compiling and solving a system of linear equations. The computational domain divided into a set of polygons, which in the simplest case have triangular cells. The geometric inverse problem of magnetostatics for electromagnetic passive shield calculated not only «geometric» position of passive screen, but also the thickness and conductivity characteristics of the passive screen. Naturally, geometric inverse problem of magnetostatics for electromagnetic passive shield is an uncorrected problem and can have many solutions. As a rule, the solution of this geometric inverse problem also comes down to solving an optimization problem and solved approximately.

Definition of geometric inverse magnetostatic problem for magnetic field combined electromagnetic silence design. Geometric inverse magnetostatic problem calculates the cause – the magnitude of source of initial magnetic field and coordinates of «geometric» location of this source at a given «geometric» point in space in such a way as to realize the effect – a given magnetic field at a given point in space. Naturally, this problem is a mathematically uncorrected problem and can have many solutions. The same given magnetic field at a given point in space can be realized using different sources of the initial magnetic field and these sources can be located at different «geometric» points in space. This problem is always solved approximately, as a rule, based on the solution of the optimization problem.

In fact, geometric inverse problem is the problem of approximating a given distribution of a magnetic field using a finite number of sought sources of a magnetic field, so that the approximation problem is parameterized in the form of power values and coordinates of the «geometric» location of the sought sources of a magnetic field.

Geometric inverse magnetostatics problem for combined electromagnetic shielding system design problem calculated spatial location and parameters of magnetic field sources to generate compensating magnetic field directed opposite to original magnetic field [20–22]. Initial magnetic field generated by power line wires and the compensating magnetic field simultaneously generated by compensating windings of active shielding system and continuous passive shield.

Consider geometrical inverse problem of magnetostatics for task of designing a combined electromagnetic screen, which consists in calculating the spatial location and parameters of magnetic field sources to generate a compensating magnetic field directed opposite to initial magnetic field [27–32]. At the same time, initial magnetic field generated by power line wires, and compensating magnetic field simultaneously generated by compensating windings of active shielding system and solid passive shield.

Consider desired parameters vector X for design of combined shielding system, components of which are geometric dimensions values vector X_a of compensating windings, as well as currents $A_{\omega i}$ and phases $\varphi_{\omega i}$ in compensating windings: as well as geometric dimensions vector X_p, thickness and material of passive shield [33–35]. In addition, we also include in desired parameters vector X sought elements of matrices A_p, B_p, C_p, D_p, determined by closed control channels PID regulators gain coefficients [36, 37].

Then, for given initial values of sought parameters vector X and uncertainty parameters vector $\boldsymbol{\delta}$ of combined shielding system designing task resulting magnetic field induction effective value $\boldsymbol{B}_R(X,\boldsymbol{\delta},P_i)$ at shielding space point Q_i calculated, based on finite element calculation system of COMSOL Multiphysics [38–41]. Then combined shielding system designing task reduced to vector game solution calculating

$$\boldsymbol{B}_R(X,\boldsymbol{\delta}) = \langle \boldsymbol{B}_R(X,\boldsymbol{\delta},P_i) \rangle. \qquad (13)$$

Game payoff vector components $\boldsymbol{B}_R(X,\boldsymbol{\delta},P_i)$ are effective values of resulting magnetic field induction at all given points P_i of shielding space. In this vector game, it is necessary to calculated payoff vector game minimum along vector X, but same payoff vector game maximum along the vector $\boldsymbol{\delta}$ [42–44].

At the same time, it is necessary to take into account restrictions on desired parameters vector X of combined shielding system in form of vector inequality and, possibly, vector equality.

$$G(X) \leq G_{\max}, \quad H(X) = 0. \qquad (14)$$

Solving problem algorithm. Components of the vector game (13) and vector constraints (14) are nonlinear functions of required parameters vector X and calculated based on finite element system of COMSOL Multiphysics.

Consider *method of solving formulated problem.* Local minimum task calculation at one point of considered space is, as a rule, multi-extreme, containing local minima and maxima, therefore, it is advisable to use stochastic multi-agent optimization algorithms for its solution. Consider calculation algorithm for Pareto-optimal solutions set of multi-criteria nonlinear programming problems based on stochastic multi-agent optimization [45]. Particle swarm optimization algorithms – PSO algorithms have been developed based on collective intelligence idea of particle swarm, such as gbest PSO and lbest PSO algorithms.

Stochastic multi-agent optimization methods application for multi-criteria problems solving causes certain difficulties and this direction continues to develop intensively. To solve original multi-criteria problem of nonlinear programming with constraints stochastic multi-agent optimization algorithm design based on particle swarms set, which number is equal to vector optimization criterion components number [46].

To increase global solution calculation speed stochastic multi-agent optimization nonlinear algorithms used, in which particle i swarm j movement described by following expressions [47]

$$v_{ij}(t+1) = w_j v_{ij}(t) + c_{1j} r_{1j}(t) H(p_{1j} - \varepsilon_{1j}(t)) \times \ldots$$
$$\ldots \times [y_{ij}(t) - x_{ij}(t)] + c_{2j} r_{2j}(t) H(p_{2j} - \varepsilon_{2j}(t)) \times \ldots \quad (15)$$
$$\ldots \times [y_j^*(t) - x_{ij}(t)]$$
$$x_{ij}(t+1) = x_{ij}(t) + v_{ij}(t+1), \quad (16)$$

where position $x_{ij}(t)$ and speed $v_{ij}(t)$ of particle i swarm j.

To global solution calculation of initial multi-criteria problem, individual swarms exchanged information among themselves during local criteria optimal solutions calculation [48]. Information about global optimum calculated by another swarm particles used to particles movement speed calculated of one swarm, which allows all potential Pareto-optimal solutions identified.

At each step t particle i swarm j movement of local solutions advantages functions calculated by all swarms used. Solution $X_j^*(t)$ calculated during objective function $B(X(t),P_j)$ optimization by swarm j is better in relation to solution $X_k^*(t)$ calculated during objective function $B(X(t),P_k)$ optimization by swarm k, i.e. $X_j^*(t) \succ X_k^*(t)$, if condition fulfilled

$$\max_{i=1,m} B\left(P_i, X_j^*(t)\right) < \max_{i=1,m} B\left(P_i, X_k^*(t)\right). \quad (17)$$

Global solution $X_k^*(t)$ calculated by swarm k used as global optimal solution $X_j^*(t)$ for swarm k, which is better in relation to global solution $X_k^*(t)$ by swarm k based on preference relationship (17).

Simulation results. Let us consider the results of calculations of resulting magnetic field in the designed combined electromagnetic combined shielding system during 3D modeling. The initial magnetic field generated by «Barrel» type double-circuit power line with wires currents $I = 26.79$ A. As result of designing combined electromagnetic shield for this power line, coordinates of two compensation windings location of active shielding

system, as well as currents magnitudes and phases in these windings, were calculated. Figure 3 shows diagram of power line wires arrangement, residential building and two compensation windings.
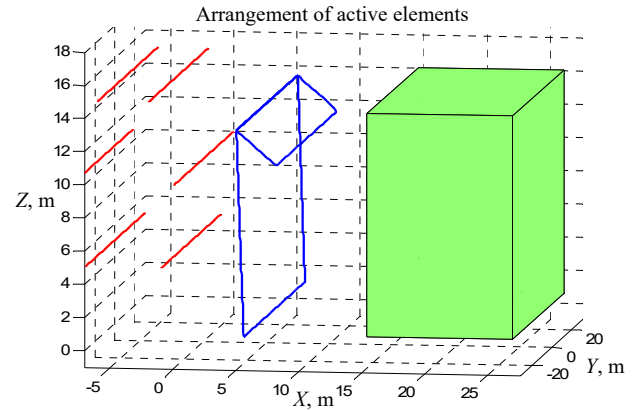

Fig. 3. Layout of power lines, residential buildings and two compensation windings

First, let's look results of 3D modeling of resulting magnetic field when combined shield operates without side plates. Figure 4 shows distribution of resulting magnetic field induction along passive screen length for various coordinates along passive shield height.
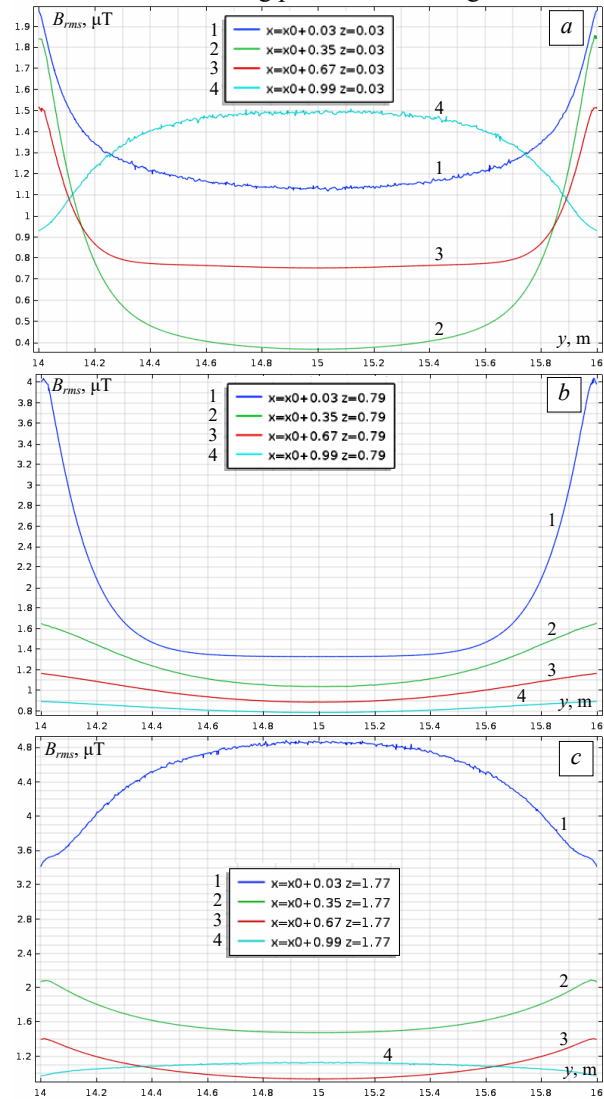

Fig. 4. Resulting magnetic field induction distribution along passive shield length

As follows from Fig. 4,*a* initial magnetic field is most effectively shield at 0.3 m height and a width of 0.35 m at center of passive shield length so that resulting magnetic field induction is 0.4 μT. At the same time, along edges of passive screen length, induction level of resulting magnetic field further increases by 4.6 times and amounts to 1.85 μT.

When approaching passive shield width to 0.03 m distance resulting magnetic induction level field increases by 2.8 times and amounts to 1.12 μT. This occurs due to an increase resulting magnetic field induction level near passive screen. At the same time, along edges of passive shield length resulting magnetic field induction level further increases by 1.7 times and amounts to 2 μT.

When moving away from passive shield by 0.99 m distance in width resulting magnetic field induction level also increases by 3.75 times and amounts to 1.5 μT. However, at passive shield length edges resulting magnetic field induction level decreases by 1.57 times and amounts to 0.92 μT.

As follows from Fig. 4,*c* highest value of resulting magnetic field induction level of 4.8 μT observed near passive shield at 0.03 m distance and at 1.17 m height. Firstly, at this height highest value of initial magnetic field induction is 2.55 μT, and, secondly, near passive screen there is an increase in initial magnetic field induction level by 1.88 times.

However, at passive screen length edges resulting magnetic field induction level decreases by 1.41 times and amounts to 3.4 μT.

Let us now consider calculations results of magnetic field generated by a double-circuit power line of the «Barrel» type with wires currents $I = 26.79$ A for combined screen in which of the passive screen side surfaces are covered with aluminum sheets.

Figure 5 shows resulting magnetic field induction distribution along the length of passive screen with side plates for various coordinates along height and width of passive screen.

Comparison resulting magnetic field induction distributions with side surfaces combined shield (Fig. 5) and without side surfaces (Fig. 4) shown that resulting magnetic field induction levels in central subsection of passive shield for these combined shield are almost the same.

However, at passive shield length edges when using side plates induction level is slightly lower. So, for example, for section at 0.3 m height and 0.35 m width at passive shield length center, where initial magnetic field is screened most effectively so that of the resulting magnetic field induction is 0.4 μT for both combination shield types.

Moreover, for combined shield without side surfaces along passive shield length edges resulting magnetic field induction level increases by 4.6 times and amounts to 1.85 μT, and when using side surfaces resulting magnetic field induction level increases only by 3.87 times and amounts to 1.55 μT.

Combined shield experimental setup. To conduct experimental studies experimental setup of combined shielding system under consideration developed. All experimental studies carried out on the magnetodynamic measuring stand at the Anatolii Pidhornyi Institute of Power Machines and Systems of the National Academy of Sciences of Ukraine [49].
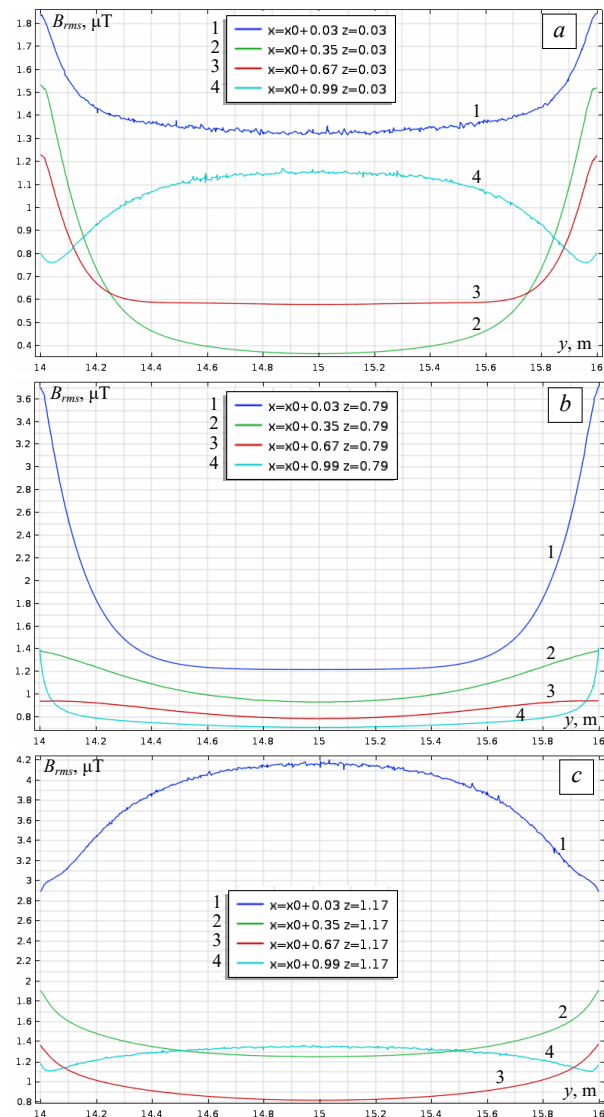

Fig. 5. Resulting magnetic field induction distribution along passive shield length with side plates

The experimental setup contains setup of double-circuit power line with six wires «Barrel» arrangement, two compensation windings of active shielding system and electromagnetic passive shield made of solid aluminum.

To conduct experimental studies of a combined shielding system, in which the side surfaces of the passive shield are open experimental setup was developed (Fig. 6).

Fig. 6. Passive shield without side plates

Two magnetic field sensors installed inside passive screen to implement two closed-loop control loops for two compensation windings of active shielding system with feedback on resulting magnetic field.

During process of adjusting control loops axes of these sensors set in such a way as to measure magnetic field induction maximum value generated by compensation winding of corresponding compensating channel. This installation of magnetic field sensors axes makes it possible to minimize the influence of channels on each other when they work together.

Two more magnetic field sensors are also installed inside passive shield, axes of which directed parallel to coordinate axes. These two sensors used in system for measuring space-time characteristics of resulting magnetic field. This measuring system used to adjust control loops of active shielding system of combined magnetic field shielding.

To power compensation windings power amplifiers used (Fig. 7).

In Fig. 8 shown combined shielding control system. To measure resulting magnetic field inside shielding space three-coordinate magnetometer type «TES 1394S triaxial ELF magnetic field meter» used with shown in Fig. 9.

This magnetometer measures three components of magnetic field induction vector using three orthogonal measuring coils (Fig. 10). Axes of these three measuring coils are orthogonal to each other and form an orthogonal coordinate system for measuring magnetic field.

Fig. 7. Power amplifiers for powering compensation windings

Fig. 8. Combination screen control system

To conduct experimental studies of combined shield, in which the side surfaces of the passive shield are covered with aluminum sheets experimental setup was developed (Fig. 11).

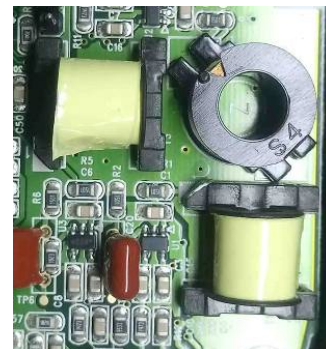Fig. 9. Three-coordinate magnetometer for measuring resulting magnetic field

Fig. 10. Measuring coils of triaxial magnetometer

Fig. 11. Experimental installation of passive shield with side plates

Experimental studies results. Let us now consider experimental studies of resulting magnetic field distributions with combined electromagnetic shield consisting of two compensation windings of active shield and electromagnetic continuous passive shield.

First, let us consider experimental studies results of resulting magnetic field when operating combined shield without side plates. Figure 12 shows experimentally measured distributions of magnetic field induction along passive shield length for various coordinates along height and width of passive shield.

By analogy with calculations results of resulting magnetic field induction shown in Fig. 4,*a*, as follows from Fig. 10,*a* initial magnetic field is most effectively shield at 0.3 m height and 0.35 m width at passive shield length center so that resulting magnetic field induction is 0.27 μT.

At the same time, along passive shield length edges resulting magnetic field induction level increases by 2.59 times and amounts to 0.7 μT.

When passive shield width approaching to 0.03 m distance resulting magnetic field induction level increases by 1.22 times and amounts to 0.33 μT. This occurs due to an increase in resulting magnetic field induction level near passive shield.

At the same time, along passive shield length edges resulting magnetic field induction level further increases by 2.12 times and amounts to 0.7 μT. When moving away from passive shield by 0.99 m distance in width resulting magnetic field induction level also increases by 2.59 times and amounts to 0.7 μT. However, at passive shield length resulting magnetic field induction level decreases edges by 1.57 times and amounts to 0.455 μT.
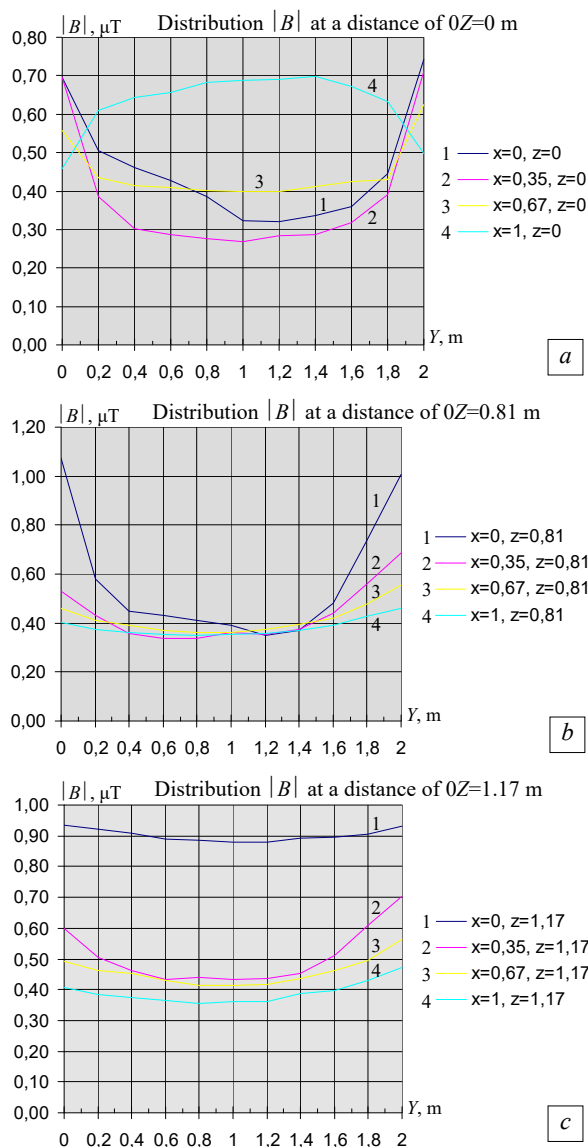
Fig. 12. Experimentally measured distributions of magnetic field induction of passive shield without side plates

Fig. 13. Experimentally measured distributions of magnetic field induction along passive shield length with side plates

As follows from Fig. 12,*c* resulting magnetic field induction level highest value of 0.88 µT observed near passive shield at 0.03 m distance and at 1.17 m height. Firstly, at this height initial magnetic field induction level is highest and, secondly, near passive shield initial magnetic field induction level increase observed.

However, at passive screen length edges resulting magnetic field induction level increases by 1.05 times and amounts to 0.93 µT.

Thus, magnetic field induction distribution change nature experimentally measured on combined shielding system installation corresponds to calculated values of resulting magnetic field induction distribution during operation of combined shield.

Let us now consider experimental measurements results of magnetic field induction on experimental installation of combined shield, in which passive shield side surfaces covered by aluminum sheets. Figure 13 shows experimentally measured distribution of resulting magnetic field induction level on experimental installation of combined shield, in which passive shield side surfaces covered by aluminum sheets.
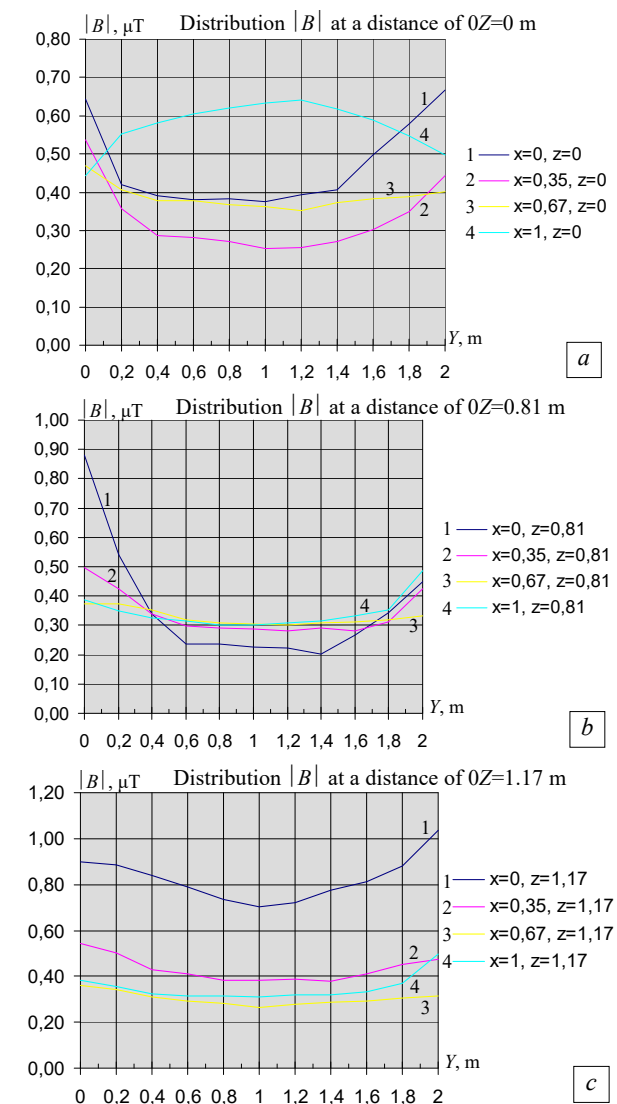
Comparison of experimentally measured distributions of resulting magnetic field induction with combined shield without side surfaces (Fig. 12) and with the side surfaces (Fig. 13) shows that resulting magnetic field induction levels in passive shield central section for these combined shield are almost the same.

However, at passive shield length edges when using side plates induction level is slightly lower. So, for example, for 0.3 m height section and for 0.35 m width at passive shield length center, where initial magnetic field is screened most effectively so that the experimentally measured resulting magnetic field induction is 0.27 µT for combination shield both types.

Moreover, for a combined shield without side surfaces along of passive shield length edges, resulting magnetic field induction level increases by 2.59 times and amounts to 0.7 µT, and when using side surfaces resulting magnetic field induction level increases only by 2.4 times and amounts to 0.65 µT.

Conclusions.

1. For the first time the method for normalization of overhead power lines magnetic field in residential building space based on optimization of combined active-passive electromagnetic shielding system for magnetic field three-dimensional model developed.

2. Optimization of combined electromagnetic shielding system for initial magnetic field three-dimensional model solved based on multi-criteria two-player antagonistic game solution. Game payoff vector calculated based on finite element calculations system COMSOL Multiphysics package. Game solution calculated based on particles multiswarm optimization algorithms.

3. During optimization of combined electromagnetic shielding system for magnetic field three-dimensional model Spatial location coordinates of shielding winding, currents and phases in shielding winding of robust active shielding system, geometric dimensions and thickness of electromagnetic passive shield calculated.

4. The results of theoretical and experimental studies of normalization for overhead power lines magnetic field by combined electromagnetic passive and active shielding system for magnetic field three-dimensional model in residential building from two-circuit overhead power transmission line with wires «Barrel» type arrangement presented. In the future, it is necessary to implement such combined electromagnetic passive and active shielding systems to normalize the field in real residential building.

Conflict of interest. The authors declare that they have no conflicts of interest.

REFERENCES

1. Sung H., Ferlay J., Siegel R.L., Laversanne M., Soerjomataram I., Jemal A., Bray F. Global Cancer Statistics 2020: GLOBOCAN Estimates of Incidence and Mortality Worldwide for 36 Cancers in 185 Countries. *CA: A Cancer Journal for Clinicians*, 2021, vol. 71, no. 3, pp. 209-249. doi: https://doi.org/10.3322/caac.21660.

2. *Directive 2013/35/EU of the European Parliament and of the Council of 26 June 2013 on the minimum health and safety requirements regarding the exposure of workers to the risks arising from physical agents (electromagnetic fields).* Available at: http://data.europa.eu/eli/dir/2013/35/oj (Accessed 20 February 2025).

3. *The International EMF Project. Radiation & Environmental Health Protection of the Human Environment World Health Organization.* Geneva, Switzerland, 1996. 2 p. Available at: https://www.who.int/initiatives/the-international-emf-project (Accessed 20 February 2025).

4. Rozov V., Grinchenko V., Tkachenko O., Yerisov A. Analytical Calculation of Magnetic Field Shielding Factor for Cable Line with Two-Point Bonded Shields. *2018 IEEE 17th International Conference on Mathematical Methods in Electromagnetic Theory (MMET)*, 2018, pp. 358-361. doi: https://doi.org/10.1109/MMET.2018.8460425.

5. Rozov V.Y., Pelevin D.Y., Kundius K.D. Simulation of the magnetic field in residential buildings with built-in substations based on a two-phase multi-dipole model of a three-phase current conductor. *Electrical Engineering & Electromechanics*, 2023, no. 5, pp. 87-93. doi: https://doi.org/10.20998/2074-272X.2023.5.13.

6. Rozov V.Y., Zavalnyi A.V., Zolotov S.M., Gretskikh S.V. The normalization methods of the static geomagnetic field inside houses. *Electrical Engineering & Electromechanics*, 2015, no. 2, pp. 35-40. doi: https://doi.org/10.20998/2074-272X.2015.2.07.

7. Rozov V.Yu., Reutskyi S.Yu., Pelevin D.Ye., Kundius K.D. Approximate method for calculating the magnetic field of 330-750 kV high-voltage power line in maintenance area under voltage. *Electrical Engineering & Electromechanics*, 2022, no. 5, pp. 71-77. doi: https://doi.org/10.20998/2074-272X.2022.5.12.

8. Salceanu A., Paulet M., Alistar B.D., Asiminicesei O. Upon the contribution of image currents on the magnetic fields generated by overhead power lines. *2019 International Conference on Electromechanical and Energy Systems (SIELMEN)*. 2019. doi: https://doi.org/10.1109/sielmen.2019.8905880.

9. Del Pino Lopez J.C., Romero P.C. Influence of different types of magnetic shields on the thermal behavior and ampacity of underground power cables. *IEEE Transactions on Power Delivery*, Oct. 2011, vol. 26, no. 4, pp. 2659-2667. doi: https://doi.org/10.1109/tpwrd.2011.2158593.

10. Hasan G.T., Mutlaq A.H., Ali K.J. The Influence of the Mixed Electric Line Poles on the Distribution of Magnetic Field. *Indonesian Journal of Electrical Engineering and Informatics (IJEEI)*, 2022, vol. 10, no. 2, pp. 292-301. doi: https://doi.org/10.52549/ijeei.v10i2.3572.

11. Victoria Mary S., Pugazhendhi Sugumaran C. Investigation on magneto-thermal-structural coupled field effect of nano coated 230 kV busbar. *Physica Scripta*, 2020, vol. 95, no. 4, art. no. 045703. doi: https://doi.org/10.1088/1402-4896/ab6524.

12. Ippolito L., Siano P. Using multi-objective optimal power flow for reducing magnetic fields from power lines. *Electric Power Systems Research*, 2004, vol. 68, no. 2, pp. 93-101. doi: https://doi.org/10.1016/S0378-7796(03)00151-2.

13. Barsali S., Giglioli R., Poli D. Active shielding of overhead line magnetic field: Design and applications. *Electric Power Systems Research*, May 2014, vol. 110, pp. 55-63. doi: https://doi.org/10.1016/j.epsr.2014.01.005.

14. Bavastro D., Canova A., Freschi F., Giaccone L., Manca M. Magnetic field mitigation at power frequency: design principles and case studies. *IEEE Transactions on Industry Applications*, May 2015, vol. 51, no. 3, pp. 2009-2016. doi: https://doi.org/10.1109/tia.2014.2369813.

15. Beltran H., Fuster V., García M. Magnetic field reduction screening system for a magnetic field source used in industrial applications. *9 Congreso Hispano Luso de Ingeniería Eléctrica (9 CHLIE)*, Marbella (Málaga, Spain), 2005, pp. 84-99.

16. Bravo-Rodríguez J., Del-Pino-López J., Cruz-Romero P. A Survey on Optimization Techniques Applied to Magnetic Field Mitigation in Power Systems. *Energies*, 2019, vol. 12, no. 7, art. no. 1332. doi: https://doi.org/10.3390/en12071332.

17. Canova A., del-Pino-López J.C., Giaccone L., Manca M. Active Shielding System for ELF Magnetic Fields. *IEEE Transactions on Magnetics*, March 2015, vol. 51, no. 3, pp. 1-4. doi: https://doi.org/10.1109/tmag.2014.2354515.

18. Canova A., Giaccone L. Real-time optimization of active loops for the magnetic field minimization. *International Journal of Applied Electromagnetics and Mechanics*, Feb. 2018, vol. 56, pp. 97-106. doi: https://doi.org/10.3233/jae-172286.

19. Canova A., Giaccone L., Cirimele V. Active and passive shield for aerial power lines. *Proc. of the 25th International Conference on Electricity Distribution (CIRED 2019)*, 3-6 June 2019, Madrid, Spain. Paper no. 1096.

20. Canova A., Giaccone L. High-performance magnetic shielding solution for extremely low frequency (ELF) sources. *CIRED - Open Access Proceedings Journal*, Oct. 2017, vol. 2017, no. 1, pp. 686-690. doi: https://doi.org/10.1049/oap-cired.2017.1029.

21. Celozzi S. Active compensation and partial shields for the power-frequency magnetic field reduction. *2002 IEEE International Symposium on Electromagnetic Compatibility*, Minneapolis, MN, USA, 2002, vol. 1, pp. 222-226. doi: https://doi.org/10.1109/isemc.2002.1032478.

22. Celozzi S., Garzia F. Active shielding for power-frequency magnetic field reduction using genetic algorithms optimization. *IEE Proceedings - Science, Measurement and Technology*, 2004, vol. 151, no. 1, pp. 2-7. doi: https://doi.org/10.1049/ip-smt:20040002.

23. Celozzi S., Garzia F. Magnetic field reduction by means of active shielding techniques. *WIT Transactions on Biomedicine and Health*, 2003, vol. 7, pp. 79-89. doi: https://doi.org/10.2495/ehr030091.

24. Martynenko G. Analytical Method of the Analysis of Electromagnetic Circuits of Active Magnetic Bearings for Searching Energy and Forces Taking into Account Control Law. *2020 IEEE KhPI Week on Advanced Technology (KhPIWeek)*, 2020, pp. 86-91. doi: https://doi.org/10.1109/KhPIWeek51551.2020.9250138.

25. Popov A., Tserne E., Volosyuk V., Zhyla S., Pavlikov V., Ruzhentsev N., Dergachov K., Havrylenko O., Shmatko O., Averyanova Y., Ostroumov I., Kuzmenko N., Sushchenko O., Zaliskyi M., Solomentsev O., Kuznetsov B., Nikitina T. Invariant Polarization Signatures for Recognition of Hydrometeors by Airborne Weather Radars. *Computational Science and Its Applications – ICCSA 2023. Lecture Notes in Computer Science*, 2023, vol. 13956, pp. 201-217. doi: https://doi.org/10.1007/978-3-031-36805-9_14.

26. Sushchenko O., Averyanova Y., Ostroumov I., Kuzmenko N., Zaliskyi M., Solomentsev O., Kuznetsov B., Nikitina T., Havrylenko O., Popov A., Volosyuk V., Shmatko O., Ruzhentsev N., Zhyla S., Pavlikov V., Dergachov K., Tserne E. Algorithms for Design of Robust Stabilization Systems. *Computational Science and Its Applications – ICCSA 2022. ICCSA 2022. Lecture Notes in Computer Science*, 2022, vol. 13375, pp. 198-213. doi: https://doi.org/10.1007/978-3-031-10522-7_15.

27. Ostroverkhov M., Chumack V., Monakhov E., Ponomarev A. Hybrid Excited Synchronous Generator for Microhydropower Unit. *2019 IEEE 6th International Conference on Energy Smart Systems (ESS)*, Kyiv, Ukraine, 2019, pp. 219-222. doi: https://doi.org/10.1109/ess.2019.8764202.

28. Ostroverkhov M., Chumack V., Monakhov E. Ouput Voltage Stabilization Process Simulation in Generator with Hybrid Excitation at Variable Drive Speed. *2019 IEEE 2nd Ukraine Conference on Electrical and Computer Engineering (UKRCON)*, Lviv, Ukraine, 2019, pp. 310-313. doi: https://doi.org/10.1109/ukrcon.2019.8879781.

29. Tytiuk V., Chornyi O., Baranovskaya M., Serhiienko S., Zachepa I., Tsvirkun L., Kuznetsov V., Tryputen N. Synthesis of a fractional-order $PI^\lambda D^\mu$-controller for a closed system of switched reluctance motor control. *Eastern-European Journal of Enterprise Technologies*, 2019, no. 2 (98), pp. 35-42. doi: https://doi.org/10.15587/1729-4061.2019.160946.

30. Chornyi O., Serhiienko S. A virtual complex with the parametric adjustment to electromechanical system parameters. *Technical Electrodynamics*, 2019, no. 1, pp. 38-41. doi: https://doi.org/10.15407/techned2019.01.038.

31. Shchur I., Kasha L., Bukavyn M. Efficiency Evaluation of Single and Modular Cascade Machines Operation in Electric Vehicle. *2020 IEEE 15th International Conference on Advanced Trends in Radioelectronics, Telecommunications and Computer Engineering (TCSET)*, Lviv-Slavske, Ukraine, 2020, pp. 156-161. doi: https://doi.org/10.1109/tcset49122.2020.235413.

32. Shchur I., Turkovskyi V. Comparative Study of Brushless DC Motor Drives with Different Configurations of Modular Multilevel Cascaded Converters. *2020 IEEE 15th International Conference on Advanced Trends in Radioelectronics, Telecommunications and Computer Engineering (TCSET)*, Lviv-Slavske, Ukraine, 2020, pp. 447-451. doi: https://doi.org/10.1109/tcset49122.2020.235473.

33. Volosyuk V., Zhyla S., Pavlikov V., Ruzhentsev N., Tserne E., Popov A., Shmatko O., Dergachov K., Havrylenko O., Ostroumov I., Kuzmenko N., Sushchenko O., Averyanova Yu., Zaliskyi M., Solomentsev O., Kuznetsov B., Nikitina T. Optimal Method for Polarization Selection of Stationary Objects Against the Background of the Earth's Surface. *International Journal of Electronics and Telecommunications*, 2022, vol. 68, no. 1, pp. 83-89. doi: https://doi.org/10.24425/ijet.2022.139852.

34. Halchenko V., Trembovetska R., Bazilo C., Tychkova N. Computer Simulation of the Process of Profiles Measuring of Objects Electrophysical Parameters by Surface Eddy Current Probes. *Lecture Notes on Data Engineering and Communications Technologies*, 2023, vol. 178, pp. 411-424. doi: https://doi.org/10.1007/978-3-031-35467-0_25.

35. Halchenko V., Bacherikov D., Filimonov S., Filimonova N. Improvement of a Linear Screw Piezo Motor Design for Use in Accurate Liquid Dosing Assembly. *Smart Technologies in Urban Engineering. STUE 2022. Lecture Notes in Networks and Systems*, 2023, vol. 536, pp. 237-247. doi: https://doi.org/10.1007/978-3-031-20141-7_22.

36. Chystiakov P., Chornyi O., Zhautikov B. Remote control of electromechanical systems based on computer simulators. *Proceedings of the International Conference on Modern Electrical and Energy Systems, MEES 2017* (2017), 2018. – January, pp. 364–367. doi: https://doi.org/10.1109/MEES.2017.8248934.

37. Zagirnyak M., Bisikalo O., Chorna O., Chornyi O. A Model of the Assessment of an Induction Motor Condition and Operation Life, Based on the Measurement of the External Magnetic Field. *2018 IEEE 3rd International Conference on Intelligent Energy and Power Systems (IEPS)*, Kharkiv, 2018, pp. 316-321. doi: https://doi.org/10.1109/ieps.2018.8559564.

38. Maksymenko-Sheiko K.V., Sheiko T.I., Lisin D.O., Petrenko N.D. Mathematical and Computer Modeling of the Forms of Multi-Zone Fuel Elements with Plates. *Journal of Mechanical Engineering*, 2022, vol. 25, no. 4, pp. 32-38. doi: https://doi.org/10.15407/pmach2022.04.032.

39. Hontarovskyi P.P., Smetankina N.V., Ugrimov S.V., Garmash N.H., Melezhyk I.I. Computational Studies of the Thermal Stress State of Multilayer Glazing with Electric Heating. *Journal of Mechanical Engineering*, 2022, vol. 25, no. 1, pp. 14-21. doi: https://doi.org/10.15407/pmach2022.02.014.

40. Kostikov A.O., Zevin L.I., Krol H.H., Vorontsova A.L. The Optimal Correcting the Power Value of a Nuclear Power Plant Power Unit Reactor in the Event of Equipment Failures. *Journal of Mechanical Engineering*, 2022, vol. 25, no. 3, pp. 40-45. doi: https://doi.org/10.15407/pmach2022.03.040.

41. Rusanov A.V., Subotin V.H., Khoryev O.M., Bykov Y.A., Korotaiev P.O., Ahibalov Y.S. Effect of 3D Shape of Pump-Turbine Runner Blade on Flow Characteristics in Turbine Mode. *Journal of Mechanical Engineering*, 2022, vol. 25, no. 4, pp. 6-14. doi: https://doi.org/10.15407/pmach2022.04.006.

42. Kurennov S., Smetankina N., Pavlikov V., Dvoretskaya D., Radchenko V. Mathematical Model of the Stress State of the Antenna Radome Joint with the Load-Bearing Edging of the Skin Cutout. *Lecture Notes in Networks and Systems*, 2022, vol. 305, pp. 287-295. doi: https://doi.org/10.1007/978-3-030-83368-8_28.

43. Kurennov S., Smetankina N. Stress-Strain State of a Double Lap Joint of Circular Form. Axisymmetric Model. *Lecture Notes in Networks and Systems*, 2022, vol 367 LNNS, pp. 36-46. doi: https://doi.org/10.1007/978-3-030-94259-5_4.

44. Smetankina N., Merkulova A., Merkulov D., Misiura S., Misiura I. Modelling Thermal Stresses in Laminated Aircraft Elements of a Complex Form with Account of Heat Sources. *Lecture Notes in Networks and Systems*, 2023, vol. 534 LNNS, pp. 233-246. doi: https://doi.org/10.1007/978-3-031-15944-2_22.

45. Ummels M. *Stochastic Multiplayer Games Theory and Algorithms*. Amsterdam University Press, 2010. 174 p.

46. Ray T., Liew K.M. A Swarm Metaphor for Multiobjective Design Optimization. *Engineering Optimization*, 2002, vol. 34, no. 2, pp. 141-153. doi: https://doi.org/10.1080/03052150210915.

47. Xiaohui Hu, Eberhart R.C., Yuhui Shi. Particle swarm with extended memory for multiobjective optimization. *Proceedings of the 2003 IEEE Swarm Intelligence Symposium*. SIS'03 (Cat. No.03EX706), Indianapolis, IN, USA, 2003, pp. 193-197. doi: https://doi.org/10.1109/sis.2003.1202267.

48. Hashim F.A., Hussain K., Houssein E.H., Mabrouk M.S., Al-Atabany W. Archimedes optimization algorithm: a new metaheuristic algorithm for solving optimization problems. *Applied Intelligence*, 2021, vol. 51, no. 3, pp. 1531-1551. doi: https://doi.org/10.1007/s10489-020-01893-z.

49. Baranov M.I., Rozov V.Y., Sokol Y.I. To the 100th anniversary of the National Academy of Sciences of Ukraine – the cradle of domestic science and technology. *Electrical Engineering & Electromechanics*, 2018, no. 5, pp. 3-11. doi: https://doi.org/10.20998/2074-272X.2018.5.01.

B.I. Kuznetsov[1], Doctor of Technical Science, Professor,
T.B. Nikitina[2], Doctor of Technical Science, Professor,
I.V. Bovdui[1], PhD, Senior Research Scientist,
K.V. Chunikhin[1], PhD, Senior Research Scientist,
V.V. Kolomiets[2], PhD, Assistant Professor,
B.B. Kobylianskyi[2], PhD, Assistant Professor
[1] Anatolii Pidhornyi Institute of Power Machines and Systems of the National Academy of Sciences of Ukraine,
2/10, Komunalnykiv Str., Kharkiv, 61046, Ukraine,
e-mail: kuznetsov.boris.i@gmail.com (Corresponding Author)
[2] Bakhmut Education Research and Professional Pedagogical Institute V.N. Karazin Kharkiv National University,
9a, Nosakov Str., Bakhmut, Donetsk Region, 84511, Ukraine.